JOURNAL OF THERMOPHYSICS AND HEAT TRANSFER
Vol. 20, No. 4, October–December 2006

Numerical Study of Heat Pipe Heat Spreaders with Large Periodic Heat Input

Gerardo Carbajal*
Rensselaer Polytechnic Institute, Troy, New York 12180
C. B. Sobhan†
National Institute of Technology, Calicut 673 601, India
and
G. P. Peterson‡
University of Colorado, Boulder, Colorado 80309

DOI: 10.2514/1.15357

The stability of a transient computational analysis of the vapor core in large flat plate heat pipe heat spreaders has been investigated using an explicit two-dimensional finite difference procedure. The calculation procedure employed a highly underrelaxed scheme to suppress instabilities arising from the transient computation of a series of interdependent, nonlinear equations that comprised the transient numerical model. Investigations were performed using various combinations of time step size and relaxation parameters, to obtain a stable, converged result. This result was then validated against a set of bulk thermodynamic calculations for the heat pipe operating under similar conditions. The computational model used an explicit scheme to minimize roundoff errors, while simultaneously overcoming the inherent instabilities occurring during the transient period of interest. The time step size and relaxation parameters for optimal and stable computation in a typical case are obtained and presented in the paper. Typical distributions of the field variables in the vapor core of large flat plate heat pipe of the type analyzed are also presented and discussed.

Nomenclature

A	=	area, m^2
c	=	specific heat, $J/kg \cdot K$
g	=	gravitational constant, m/s^2
H	=	vapor core height, m
h	=	convection heat transfer coefficient, $W/m^2 \cdot K$
h_{fg}	=	latent heat of vaporization, J/kg
k	=	thermal conductivity, $W/m \cdot K$
m''	=	mass flux, $kg/s \cdot m^2$
P	=	pressure, Pa
q''	=	heat flux, W/m^2
q	=	net heat transfer rate, W
R	=	vapor gas constant, $J/kg \cdot K$
T	=	temperature, K
t	=	time, s
u	=	x-velocity component, m/s
V	=	volume of the wall and wick combination in an element around the nodal point, m^3
v	=	y-velocity component, m/s
W	=	vapor core width, m
X	=	node number in the x-direction
x	=	axial direction, axial distance, m
Y	=	node number in the y-direction
y	=	width direction, width, m
Γ	=	convective term [Eq. (14)]
δ	=	thickness, m
Λ	=	relaxation factor
μ	=	dynamic viscosity, $Pa \cdot s$
ρ	=	density, kg/m^3

Subscripts

c	=	condenser
conv	=	convection
d	=	divergence
e	=	evaporator
g	=	saturated vapor
in	=	input
o	=	initial (reference) value
out	=	output
s	=	step size
sat	=	saturation
T	=	temperature
u	=	u-velocity
v	=	v-velocity
wall	=	wall material
wick	=	wick material
x	=	width direction
y	=	axial direction
ρ	=	density
1	=	one cycle of operation
∞	=	ambient condition

Received 5 January 2005; revision received 9 July 2005; accepted for publication 12 July 2005.

*Ph.D. Candidate, Department of Mechanical, Aerospace and Nuclear Engineering.
†Department of Mechanical Engineering; Visiting Assistant Professor, Department of Mechanical, Aerospace and Nuclear Engineering, RPI, Troy, NY.
‡Professor, Department of Mechanical Engineering and Chancellor.

Introduction

DUE to the complex nature of the thermodynamic and heat transfer processes, heat pipes present a physical system that imposes a number of difficulties when analyzed using conventional computational methods. Further complications and constraints are imposed on the modeling and solution procedures in transient analysis where high degrees of accuracy are required and equilibrium assumptions are not valid. In these situations, it is not practical to assume temperature uniformity in the vapor core of the heat pipe, as the system passes through a series of unsteady-state processes, and the heat storage by the wall and the wick of the heat pipe becomes

significant compared to the phase change heat transport. Further, the mass addition to and rejection from the vapor core, caused by vaporization and condensation in the evaporator and condenser, respectively, make necessary the determination of transient and spatial vapor density variations during the unsteady-state process.

The liquid-vapor interface is governed by the phase change process, which makes it necessary to solve the governing thermodynamic equations along with the flow and energy equations of the working fluid. In the finite difference method, the selection of a suitable numerical scheme often presents some challenges, as the number and nature of the equations can impact the stability of the solution process and may lead to problems with convergence. The domain that is most affected by such instabilities is the vapor core, as the mutual dependence of the temperature, pressure, and density is much stronger in the vapor phase than in the liquid flow in the wick.

In transient finite difference analyses, it is often better to use an explicit solution method to avoid roundoff errors and enhance the accuracy of the time-dependent solutions [1]. This is often not possible, however, due to the stability requirements and associated restrictions imposed by the time step size. Whereas implicit schemes are inherently more stable, in the simultaneous solution of complex nonlinear governing equations, the implicit scheme may still diverge unless special solution methods using small time steps are employed. In the present analysis, a method to obtain convergence is developed using an explicit scheme. This is accomplished by using successive underrelaxation [1,2] with extremely small underrelaxation parameters for updating the field variables, which avoids divergence of the explicit scheme. The optimal combination of the spatial grid size, time step size and relaxation factors can be obtained by benchmarking the results with experimental data. Once developed, this solution technique can be used to conduct parametric studies of the overall heat pipe system. The following section describes the computational schemes used in the analysis of the vapor core of a large plate heat pipe with a highly nonuniform heat input at the evaporator.

Review of Literature

The use of heat pipes as highly efficient transport devices and/or heat spreaders has found widespread applications, since first introduced in the mid-sixties. To facilitate this use a number of computational studies have been developed to analyze and optimize heat pipe design. A comprehensive review of these modeling efforts and in particular of the application of nonconventional heat pipes can be found in [3].

Although many of the reported investigations pertain to the analysis of heat pipes designed for cooling electronic packages, some of the research has also focused on the vapor flow analysis in large heat pipes. One of the earliest analyses of the vapor flow in heat pipes was presented by Cotter [4], where a one-dimensional analysis of laminar, steady, incompressible flow was performed for a cylindrical heat pipe. Analyses and parametric studies of the vapor flow in circular cross section heat pipes have been performed by Bankston and Smith [5] and in flat heat pipes by Van Ooijen and Hoogendoorn [6]. Faghri [7,8] presented numerical studies of the vapor flow in concentric double walled heat pipes, and Chen and Faghri [9] numerically analyzed the effects of single and multiple heat sources using a model which included compressibility effects in the vapor, and wall conduction. A two-dimensional numerical model was used in the analysis of the startup of flat heat pipes by Issacci et al. [10]. The compressible flow of vapor in the transient state was analyzed using a one-dimensional model by Jang et al. [11], and the numerical results were compared with experimental results. A transient two-dimensional heat pipe model was presented by Tournier and El-Genk [12], whereas Wang and Vafai [13] used analytical models to predict the transient performance of a flat plate heat pipe during startup and shutdown. Vadakkan et al. [14] investigated numerically the transient performance of a flat plate heat pipe for large input heat fluxes and high wick thermal conductivities. An experimental and theoretical approach for analyzing the transient behavior of flat plate heat pipes was developed by Xuan et al. [15] to study the effects of the working fluid charge, the thickness of the porous medium, and the orientation on the performance of the heat pipe.

Whereas these models and investigations all provide some insight into the operation and performance of various types of heat pipes, relatively few investigations have been conducted on the transient performance of flat plate heat pipes, and in most of the applications reviewed in this section, the heat pipes are modeled for their steady-state operation.

The Physical Model

The heat pipe analyzed in the present study is designed for an application as a heat spreader, in which a large heat transfer rate is periodically imposed on the front surface of the evaporator, the maximum load being 6 MW. The front surface is assumed to be subjected to an arbitrary one-dimensional heat flux distribution, as shown in Fig. 1. In the present analysis, this distribution is taken as parabolic, as given in Fig. 2. The schematic shown in Fig. 1 also illustrates the approximate physical dimensions of the heat pipe under analysis. The flat plate heat pipe functions as a heat spreader for distributing the heat flux uniformly over the rear surface, where it is dissipated from the system. The heating portion of the cycle lasts

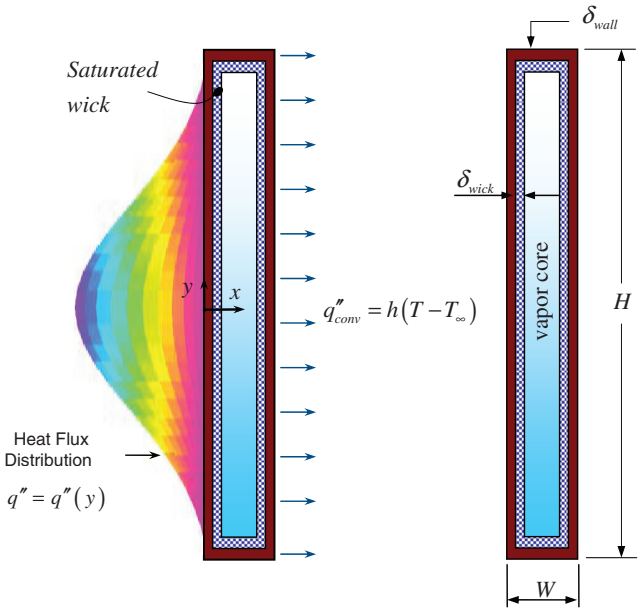

Fig. 1 The heat flux distribution on the flat plate heat pipe.

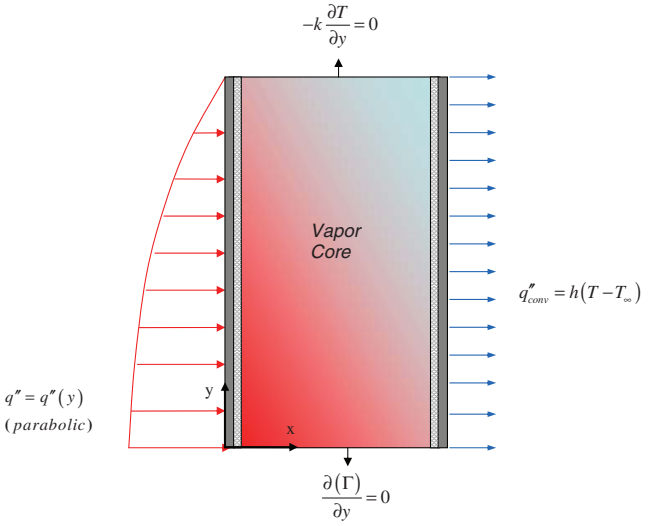

Fig. 2 Domain of analysis of the vapor core and the boundary conditions.

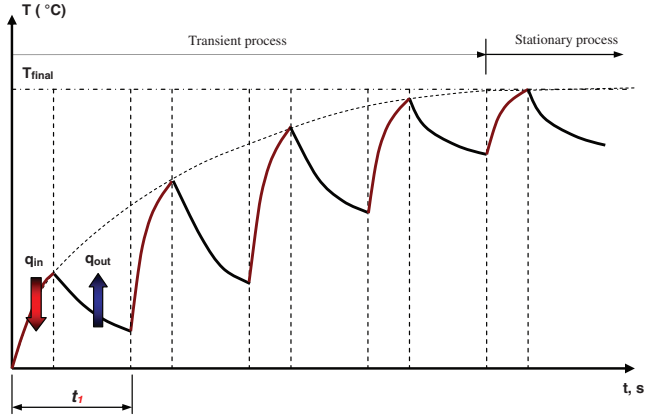

Fig. 3 Heating and cooling cycles during continuous operation.

only for 30 s, after which the heat source is removed. Figure 3 represents the pattern of the temperature variation during the heating and cooling processes in the plate heat pipe under continuous repetitive operation. The model developed herein analyzes the transient response of the vapor core in the heating portion of one cycle of operation of the heat pipe to understand the variations in temperature, pressure, and velocity of the vapor. Whereas the computation presented here corresponds to the heating portion of the first period, q_{in} in the one cycle of operation illustrated in Fig. 3, the numerical code developed is general, and can be used in analyzing the subsequent heating periods also, by appropriately incorporating the initial conditions.

The dimensions of the heat pipe under analysis correspond to the design requirements for particular special application. The maximum values permitted in this design, for the height, width, wall-thickness, and wick thickness are 4.5 m, 0.10 m, 0.004 m, and 0.008 m, respectively. These dimensions are used in the baseline case analyzed and presented in this paper. Table 1 gives the constructional details and the thermophysical properties of the system under analysis.

The heat pipe analyzed is large in dimensions, and transports a large, periodic thermal load. Because of the large mass of the system, a considerable portion of the applied heat is stored in the body of the heat pipe during the transient period. This requires that the vapor core analysis be based on transient governing equations. An assumption of uniform temperature in the vapor core will not be valid under transient operation, making it necessary to solve the energy equation in the vapor along with the fluid flow equations. The interfacial mass flux between the wick and the core is computed based on an energy balance, using a lumped parameter analysis of the wall and the wick material at the interfacial nodal locations. This procedure allows the numerical instabilities occurring in the computation of the vapor field to be better observed and analyzed. The work is aimed at detecting and resolving the stability problems in the computational scheme for the vapor core only; the study is being coupled at present to a complete model including the heat pipe wall and wick.

The density field in the vapor core varies with respect to time due to mass addition at the evaporator side and mass rejection in the condenser side of the domain. These phenomena are incorporated in the model by formulating the problem using the continuity equation, solved simultaneously with the momentum and energy equations, written in the conservative form, as suggested in the literature [14]. To relate between the pressure and temperature in the vapor, the ideal gas equation of state is used, with an assumption of constant values for the thermal conductivity, specific heat, and dynamic viscosity of the medium.

The mathematical modeling of the problem is described next, along with the domain of analysis and the boundary conditions. Because of the symmetry of the physical domain in the y-direction, the height of the domain of computation is taken as half that of the physical domain (see Fig. 2).

Governing Equations

The governing equations solved are the two-dimensional transient equations of momentum and energy conservation, along with the continuity equation. The equations, written in the conservative form, are given next, indicating their roles in the solution procedure [1,13].

The continuity equation for computation of the density field:

$$\frac{\partial \rho}{\partial t} + \frac{\partial (\rho u)}{\partial x} + \frac{\partial (\rho v)}{\partial y} = 0 \tag{1}$$

The momentum equations for the computation of the velocity components:

x-momentum equation for computing u:

$$\frac{\partial}{\partial t}(\rho u) + \frac{\partial}{\partial x}(\rho u u) + \frac{\partial}{\partial y}(\rho u v) = -\rho g_x - \frac{\partial P}{\partial x} + \mu\left(\frac{\partial^2 u}{\partial x^2} + \frac{\partial^2 u}{\partial y^2}\right) \tag{2}$$

y-momentum equation for computing v:

$$\frac{\partial}{\partial t}(\rho v) + \frac{\partial}{\partial x}(\rho u v) + \frac{\partial}{\partial y}(\rho v v) = -\rho g_y - \frac{\partial P}{\partial y} + \mu\left(\frac{\partial^2 v}{\partial x^2} + \frac{\partial^2 v}{\partial y^2}\right) \tag{3}$$

The energy equation for computing the temperature field:

$$\frac{\partial}{\partial t}(\rho c T) + \frac{\partial}{\partial x}(\rho c T u) + \frac{\partial}{\partial y}(\rho c T v) = k\left(\frac{\partial^2 T}{\partial x^2} + \frac{\partial^2 T}{\partial y^2}\right) \tag{4}$$

The equation of state for the ideal gas is used to calculate the pressure:

$$P = \rho R T \tag{5}$$

Boundary Conditions

The interfacial density, mass flux, and temperature conditions at the evaporator boundary can be expressed as follows:

At $x = 0,\ 0 \le y \le H/2$

$$\rho = \rho(T) \tag{6}$$

$$m''_e h_{\text{fg}} = -k \left.\frac{\partial T}{\partial x}\right|_{x=0}, \qquad v = 0 \tag{7}$$

$$\rho c V \frac{\mathrm{d}T}{\mathrm{d}t} = A_e q''(y) - m''_e A_e h_{\text{fg}} \tag{8}$$

The conditions at the condenser boundary are

At $x = W,\ 0 \le y \le H/2$

$$\rho = \rho(T)$$

$$m''_c h_{\text{fg}} = -k \left.\frac{\partial T}{\partial x}\right|_{x=W}, \qquad v = 0 \tag{9}$$

Table 1 Details of the heat pipe system under analysis

	k, W/m · K	c, kJ/kg · K	ρ, kg/m^3	ρc, J/m^3 · K
Properties of water vapor	0.0204	1422.76	0.0436	——
Properties of aluminum (wall)	237	903	2702	——
Properties of aluminum (wick)	——	——	——	3,461,000

$$\rho c V \frac{\partial T}{\partial t} = m''_c A_c h_{fg} - h A_c (T - T_\infty) \tag{10}$$

Equations (8) and (10) are implemented with an assumption that the wall-wick combination acts as a lumped system. An elemental volume is taken around the nodal point on the boundary of the vapor core, and the energy balance is performed using volume based weighted average values for the density and the specific heat of the wall and the wick.

Other boundary conditions can be expressed as follows:

Top boundary:

at $0 \le x \le W$, $y = H/2$

$$\left.\frac{\partial T}{\partial x}\right|_{y=H/2} = 0 \tag{11}$$

$$u = 0, \qquad v = 0 \tag{12}$$

$$\frac{\partial \rho}{\partial y} = 0 \tag{13}$$

and

Line of symmetry:

at $0 \le x \le W$, $y = 0$

$$\frac{\partial(\Gamma)}{\partial y} = 0 \tag{14}$$

where Γ represents the convective terms in the y-direction for the continuity, momentum, and energy equations (ρu, $\rho u v$, and $\rho c v T$).

Initial Conditions

It is assumed that the vapor is initially saturated, with a uniform temperature and pressure field. It is also assumed that the fluid is initially at rest.

At $t = 0$

$$T_0 = 37.78^\circ\text{C}, \qquad P = P_{sat}(T_0), \qquad \rho = \rho_g(T_0) \tag{15}$$

$$u = v = 0 \tag{16}$$

Numerical Solution

Computational Scheme

An important objective of the present work is the determination of the variations in the temperature, pressure, and velocity fields of the vapor in the early transient state, as the heating cycle is such that the system never achieves a steady-state condition. This is expected, due to the large mass of the heat pipe system, and the application of the heat load only for 30 s. To capture the transient variations without roundoff errors, and to ensure that the computational scheme is simple and straightforward, an explicit computation procedure was used. The physical domain was discretized using a mesh of 20×500. Unequal grid sizes were used in the x- and y-directions, which corresponded to the respective dimensions of the heat pipe. This produced a spatial grid size of 0.0228 mm in the x-direction and 0.312 mm in the y-direction. Using a trial and error procedure to overcome instabilities in the computation, the time step size was selected, and computations were performed using successive underrelaxation, as described in the following section, to obtain stable, converged results based on a grid refinement procedure.

Successive Underrelaxation

The explicit computation procedure introduces restrictions in the time step size due to the stringent stability criteria associated with numerical computation [1]. This results in a very small time step, which makes the computation procedure lengthy in real time. In a theoretical study using a one-dimensional transient model for a heat pipe application, Bystrov and Goncharov [16] have shown that the time steps in the numerical calculations that are necessary to satisfy stability requirements were of the order of 10^{-7} s. To use a simple explicit scheme with the present system of equations, a computational procedure was developed using successive underrelaxation, with extremely small relaxation factors. It was found that reductions in the relaxation factor could result in a stable solution with time step sizes of 10^{-5} s, allowing the transient period to be analyzed within a reasonable computation time. It was found that the velocity computations were extremely susceptible to numerical instabilities, and required very small relaxation factors as small as 10^{-8} to be used, whereas the relaxation factors required for the temperature computations were in the range 0.2–0.8. Successive underrelaxation was applied to all the field variables systematically, and their influence on the stability was studied. The method followed in the application of underrelaxation for explicit solution of the unsteady equations is as explained by Patankar [2]. Constant values of relaxation factors were used for each individual variable. At every step of numerical computation, the procedure allows only partial use of the current values of the magnitudes of the computed variables depending on the relaxation factor, the other part being substituted from the previous computation, thus bringing down the possibility of divergence. Thus, the underrelaxation technique allows the computed field variable to change only by a fraction of the difference between the new and old computed values The best combinations of relaxation factors and the time step size were obtained by performing systematic trials.

Table 2 Influence of relaxation factor Λ_T on the stability of the computational scheme ($\Lambda_u = 10^{-9}$, $\Lambda_v = 10^{-8}$, $\Lambda_\rho = 1.0$)

Time step, s	Time at divergence, s		
	$\Lambda_T = 2 \times 10^{-1}$	$\Lambda_T = 3 \times 10^{-1}$	$\Lambda_T = 4 \times 10^{-1}$
1.0×10^{-1}	3.99×10^{-4}	1.00×10^{-3}	3.99×10^{-4}
1.0×10^{-2}	2.70×10^{-3}	3.00×10^{-3}	2.80×10^{-3}
1.0×10^{-3}	2.99×10^{-2}	2.40×10^{-2}	2.28×10^{-2}
1.0×10^{-4}	1.80×10^{-1}	1.41×10^{-1}	1.20×10^{-1}
1.0×10^{-5}	8.20×10^{-1}	6.44×10^{-1}	5.50×10^{-1}
1.0×10^{-6}	4.45×10^{0}	3.94×10^{0}	3.11×10^{0}
1.0×10^{-7}	2.57×10^{1}	2.48×10^{1}	1.60×10^{1}

Table 3 Influence of relaxation factor Λ_V on the stability of the computational scheme ($\Lambda_u = 10^{-9}$, $\Lambda_T = 0.3$, $\Lambda_\rho = 1.0$)

Λ_V	Time step size, s	Time at divergence, s
1.0×10^{-6}	1.0×10^{-2}	0.31
	3.0×10^{-3}	0.51
	1.0×10^{-3}	1.30
	5.0×10^{-4}	2.50
	2.0×10^{-4}	6.06
	1.0×10^{-4}	12.30
	5.0×10^{-5}	27.05
1.0×10^{-7}	1.0×10^{-2}	1.40
	8.0×10^{-3}	1.60
	5.0×10^{-3}	2.40
	4.0×10^{-3}	3.20
	2.0×10^{-3}	6.00
	1.0×10^{-3}	12.40
	5.0×10^{-4}	26.65
1.0×10^{-8}	5.5×10^{-2}	0.31
	2.0×10^{-2}	0.51
	1.0×10^{-2}	1.30
	5.5×10^{-3}	2.50
	5.0×10^{-3}	6.06
	4.2×10^{-3}	12.30
1.0×10^{-9}	5.5×10^{-2}	0.31
	3.0×10^{-2}	0.51
	2.0×10^{-2}	1.30

Dependence of Stability on the Relaxation Parameters

The influence of the time step sizes and relaxation factors used in the investigation on the stability of the scheme are discussed in this section. It was found that the stability of the scheme was largely dependent on the relaxation factor, with smaller values yielding more stable results and moving the computation forward for a larger transient period without divergence. Representative temperature values in the domain were used as indicators of divergence of the computational scheme. Tables 2 and 3 give some of the combinations of the time step size and the relaxation parameters for temperature and v-velocity which were tried out, showing their influence on the stability. Table 2 shows the time instant where divergence occurred, while using various values of the relaxation factors for temperature computations, in combination with different time step sizes, while the other field variables were kept constant. Similarly, Table 3 gives an account of the influence of the relaxation factor for the v-velocity, in combination with different time step sizes, while the other relaxation factors were kept constant. By suitably selecting the combinations of the time step size and the relaxation factors, it was possible to overcome the instabilities in the field variables for a transient period of 30 s, which is the timeframe of interest in the current problem. A systematic refinement of the spatial grids was then used to yield converged results for the field variables in this transient period.

Figures 4 and 5 also illustrate the effect of the relaxation factors on the stability of the scheme. As understood from these plots, the relaxation parameter for the v-velocity has a greater influence on the stability than the relaxation parameter for temperature. From the computational analysis it was found that the relaxation parameter for density does not play any significant role in the stability of the scheme.

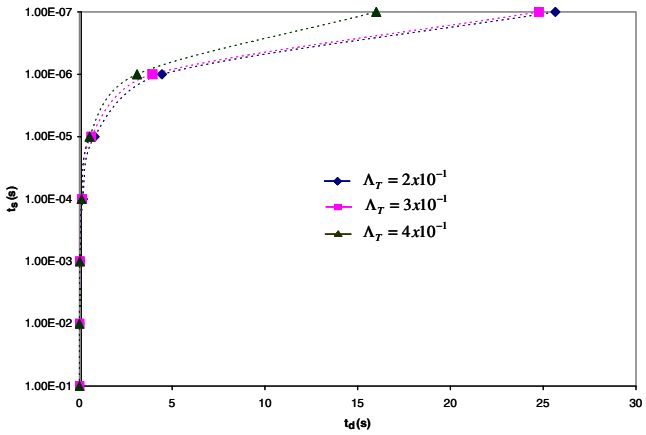

Fig. 4 Effect of the relaxation factor Λ_T and the time step size on divergence.

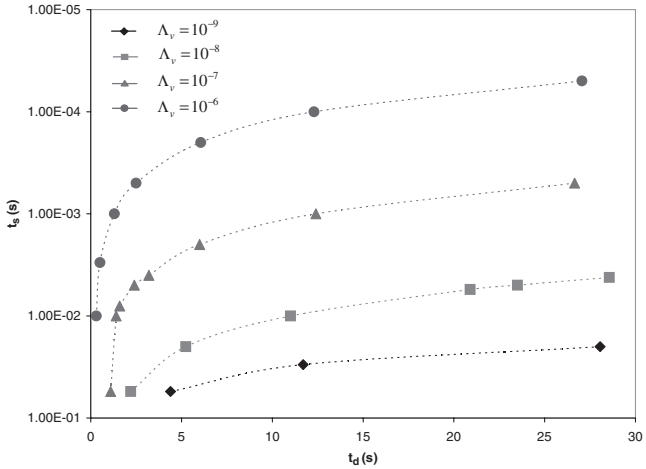

Fig. 5 Effect of the relaxation factor Λ_v and the time step size on divergence.

Validation of Computational Results

As part of the design optimization of the heat pipe, a thermodynamic calculation procedure was performed to determine the average values of the fluid properties during its operation, using the heat pipe dimensions listed in Table 1, under typical operating conditions. A quasi-equilibrium process was assumed in this analysis, assuming saturated liquid and vapor and prescribing the initial condition, to obtain the final condition at the end of a short period (5 s). This calculation was performed repetitively for equal time intervals. From the final thermodynamic state of the vapor at the end of each of these intervals, the bulk temperature was obtained using the thermodynamic tables. The temperature values in the vapor that resulted from this calculation correspond to the physical dimensions of the numerically analyzed heat pipe and were used to validate the computational results. This comparison is presented in Fig. 6. In the early transient period (that is, the first 6 s) the numerical results are found to agree very well with the corresponding results of the thermodynamic calculation. One reason for the increasing

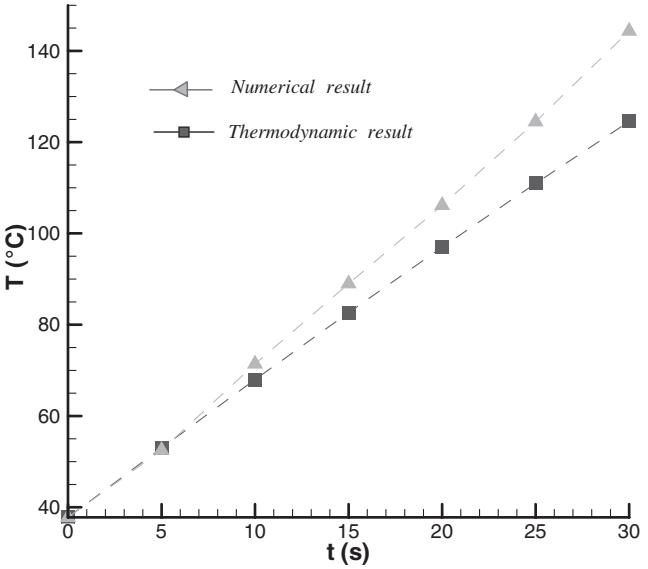

Fig. 6 Validation of the computational results by comparison with results from thermodynamic calculations.

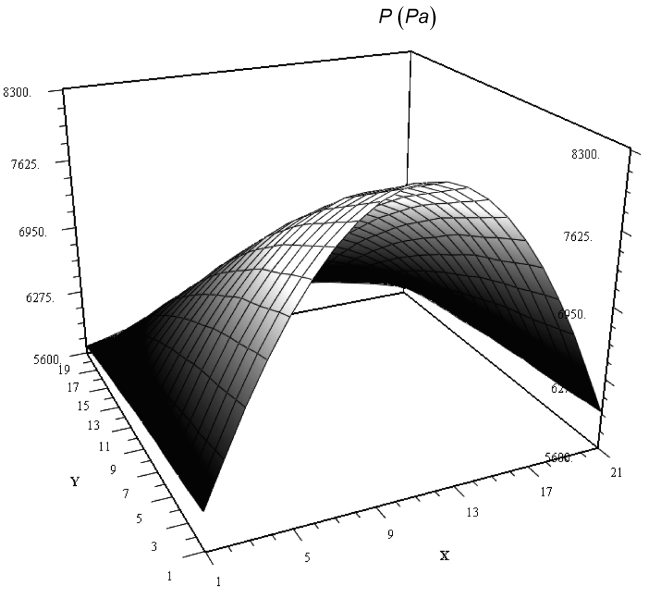

Fig. 7 The pressure distribution in the system at $t = 15$ s.

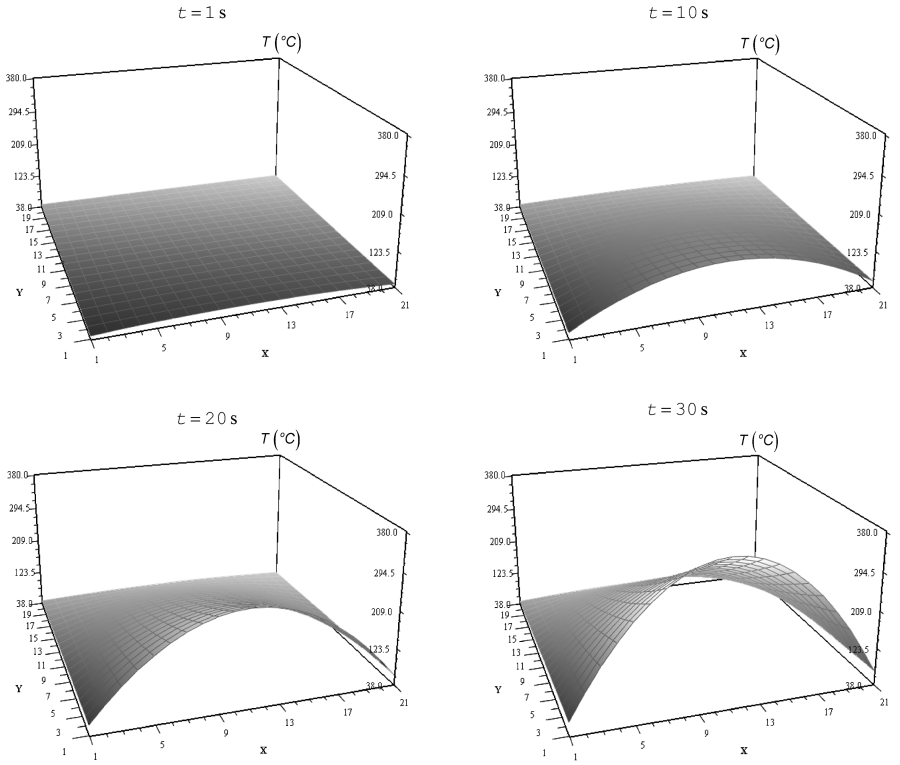

Fig. 8 The transient variation of the temperature field in the vapor core.

deviation as a function of time is the assumption of quasi-equilibrium conditions in the thermodynamic calculations. This deviation can also be attributed to the local nonuniformity of the vapor temperature, which is not considered in the thermodynamic calculations. This effect becomes more significant as the process progresses in time.

Numerical Results and Discussion

The objective of the present computational analysis, apart from developing a stable numerical scheme, was also to obtain the temperature, pressure, and velocity distributions in the vapor core of the heat pipe, which can then be incorporated into a complete analysis of the vapor, wick, and wall of the heat pipe. Among the three distinct regions of the heat pipe, the vapor core, the wick, and the wall, it is the vapor core analysis that presents the biggest computational challenge because of the density variations and the significant spatial distribution of the fluid velocity.

The numerical results of the temperature, pressure, and velocity distributions from the transient vapor core analysis for the conditions given in Table 1 are presented in Figs. 7–10. Figure 7 indicates that the pressure field has maximum values at locations corresponding to the region where the heat flux values are largest, at the center of the evaporator surface. Figure 8 illustrates the temperature distribution in the vapor core at various time instants. At the condenser side, the temperature distribution is nearly uniform, indicating that the heat pipe acts as an effective hear spreader, producing a nearly uniform

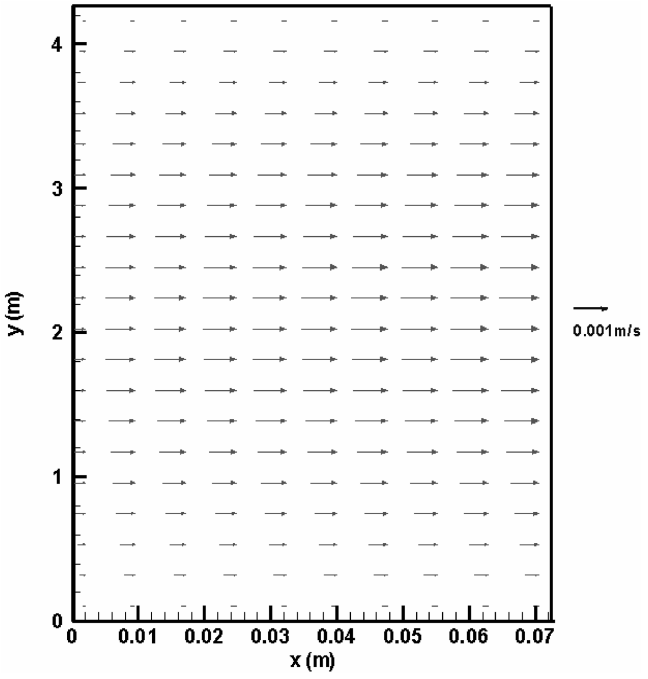

Fig. 9 The velocity vector plot for the vapor core at $t = 15$ s.

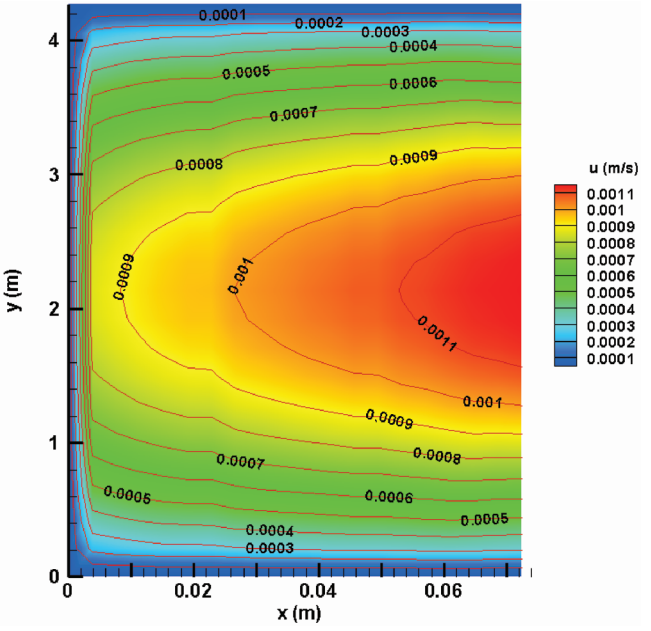

Fig. 10 Contour plot of the u-velocity field in the vapor core at $t = 15$ s.

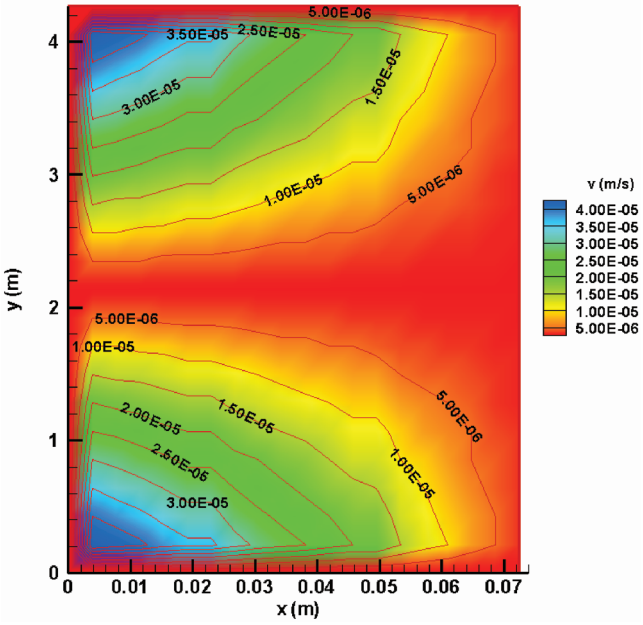

Fig. 11 Contour plot of the v-velocity field in the vapor core at $t = 15$ s.

temperature all over the condenser surface. This effect can enhance the heat dissipation from the condenser surface to a large extent, compared with the use of a metallic heat sink, as the whole condenser surface is actively used in heat dissipation. Figure 9 gives a vector plot of the resultant velocities in the vapor core, corresponding to a typical time instant (15 s) in the transient period. It is clear that the largest vapor velocities occur in the central region of the vapor core. The distributions of the individual vapor velocity components in the vapor core are also shown as contour plots in Figs. 10 and 11. It should be noted that the magnitudes of the transient velocities are much smaller compared with the predicted average values at steady-state operation, which can be computed from a steady-state energy balance between the heat input and the latent heat transfer (the value is calculated to be around 4.55 m/s at the steady state, for the highest heat flux). This is expected, as the analysis deals with the early transient period, and the velocities are only starting to grow in magnitude, due to the energy storage effect during this transient period.

Conclusion

An explicit two-dimensional finite difference model was developed to perform a transient analysis of the vapor core of a large flat plate heat pipe heat spreader, designed to handle periodic, nonuniform heat fluxes at very high heat transfer rates. The heat pipe analyzed in the problem was subjected to a nonuniform and periodic heat flux distribution at the evaporator section. It was found that, using an underrelaxation procedure with appropriate combinations of small relaxation factors and time step sizes, the instabilities in explicit time stepping could be overcome to give stable results of the field variables, during the transient period of operation. The computational model was validated against thermodynamic calculations for a typical case of the heat pipe design. The influence of the time step size and the relaxation parameters on the stability of the computational scheme was investigated, and an optimal combination was obtained to yield stable, converged results based on a successive spatial grid refinement. Distributions of the field variables obtained from the computational analysis of the vapor core of the heat pipe were also presented and discussed. The analysis presented can be used to perform parametric studies on the vapor core dimensions. The computational results indicated that the heat pipe can operate as an effective heat spreader giving an almost uniform temperature at the condenser face, while subjected to a nonuniform heat flux distribution at the evaporator face.

Acknowledgment

The authors would like to acknowledge the support of the Office of Naval Research Grant ONR N000140010454.

References

[1] Anderson, J. D., *Computational Fluid Dynamics*, The Basics with Applications, McGraw–Hill, New York, 1995, Chaps. 2, 6.
[2] Patankar, S. V., *Numerical Heat Transfer and Fluid Flow*, Hemispher, New York, 1980.
[3] Garimella, S. V., and Sobhan, C. B., "Recent Advances in the Modeling and Applications of Nonconventional Heat Pipes," *Advances in Heat Transfer*, Vol. 35, Academic Press, New York, 2001, pp. 249–308.
[4] Cotter, T. P., "Theory of Heat Pipes," Los Alamos Scientific Laboratory Report No. LA-3246-MS, 1965.
[5] Bankston, C. A., and Smith, H. J., "Vapor Flow in Cylindrical Heat Pipes," *Journal of Heat Transfer*, Vol. 95, Series C, No. 3, 1973, pp. 371–376.
[6] Van Ooijen, H., and Hoogendoorn, C. J., "Vapor Flow Calculations in a Flat Heat Pipe," *AIAA Journal*, Vol. 17, No. 11, 1979, pp. 1251–1259.
[7] Faghri, A., "Vapor Flow Analysis in a Double-Walled Concentric Heat Pipe," *Numerical Heat Transfer*, Vol. 10, No. 6, 1986, pp. 583–595.
[8] Faghri, A., "Performance Characteristics of a Concentric Annular Heat Pipe: Part 2—Vapor Flow Analysis," *Journal of Heat Transfer*, Vol. 111, No. 4, 1989, pp. 851–857.
[9] Chen, M. M., and Faghri, A., "Analysis of the Vapor Flow and the Heat Conduction Through the Liquid-Wick and Pipe Wall in a Heat Pipe with Single or Multiple Heat Sources," *International Journal of Heat and Mass Transfer*, Vol. 33, No. 9, 1990, pp. 1945–1955.
[10] Issacci, F., Catton, I., and Ghoniem, N. M., "Vapor Dynamics of Heat Pipe Start-Up," *Journal of Heat Transfer*, Vol. 113, No. 4, 1991, pp. 985–994.
[11] Jang, J. H., Faghri, A., and Chang, W. S., "Analysis of the One-Dimensional Transient Compressible Vapor Flow in Heat Pipes," *International Journal of Heat and Mass Transfer*, Vol. 34, No. 8, 1991, pp. 2029–2037.
[12] Tournier, J.-M., and El-Genk, M. S., "Heat Pipe Transient Analysis Model," *International Journal of Heat and Mass Transfer*, Vol. 37, No. 5, 1994, pp. 753–762.
[13] Wang, Y., and Vafai, K., "Transient Characterization of Flat Plate Heat Pipes During Startup and Shutdown Operations," *International Journal of Heat and Mass Transfer*, Vol. 43, No. 15, 2000, pp. 2641–2655.
[14] Vadakkan, U., Murthy, J. Y., and Garimella, S. V., "Transient Analysis of Flat Heat Pipes," American Society of Mechanical Engineers Paper HT2003-47349, 2003.
[15] Xuan, Y., Hong, Y., and Li, Q., "Investigation on Transient Behaviors of Flat Plate Heat Pipes," *Experimental Thermal and Fluid Science*, Vol. 28, Nos. 2–3, 2004, pp. 249–255.
[16] Bystrov, P. I., and Goncharov, V. F., "Starting Dynamics of High-Temperature Gas-Filled Heat Pipes," *High Temperature*, Vol. 21, No. 6, 1983, pp. 927–936.